

RECEIVED BY OSTI

OCT. 28 1985

CONF-8509185-1
BNL 37073

TO BE PRESENTED AT
CLIFF SHULL CEREMONIAL CONFERENCE
AT MIT, CAMBRIDGE, SEPT.24, 1985
- TO BE PUBLISHED IN PHYSICA B. -

BNL--37073

DE86 001733

"MAGNETIC EXCITATIONS AND POLARIZED NEUTRONS"

G. SHIRANE

HAHN-MEITNER-INSTITUTE, BERLIN and
BROOKHAVEN NATIONAL LAB., UPTON, NY.

We review the historical development of polarized beam techniques for studies of condensed matter physics. In particular we describe, in some detail, the recent advance of the triple axis technique with polarization analysis. It is now possible to carry out quantitative characterization of magnetic cross sections $S(Q, \omega)$, in absolute units, for a wide range of energy and momentum transfers. We will discuss some examples of recent inelastic measurements on 3d ferromagnets and heavy Fermions.

MASTER

Jaw

DISCLAIMER

This report was prepared as an account of work sponsored by an agency of the United States Government. Neither the United States Government nor any agency thereof, nor any of their employees, makes any warranty, express or implied, or assumes any legal liability or responsibility for the accuracy, completeness, or usefulness of any information, apparatus, product, or process disclosed, or represents that its use would not infringe privately owned rights. Reference herein to any specific commercial product, process, or service by trade name, trademark, manufacturer, or otherwise does not necessarily constitute or imply its endorsement, recommendation, or favoring by the United States Government or any agency thereof. The views and opinions of authors expressed herein do not necessarily state or reflect those of the United States Government or any agency thereof.

I. INTRODUCTION

Polarized neutron scattering has been widely utilized for condensed matter Physics since 1950's. The first application was the study of spin density distributions in ferromagnets, following the pioneering work of Shull and Nathans (1). This technique requires only a double axis configuration, without analyzer, and the magnetic scattering length p is scaled to the nuclear length b by the flipping ratio R

$$R = \frac{(b + p)^2}{(b - p)^2} \quad (1)$$

This simple technique has turned out to be an extremely sensitive way to measure p ; thus small induced moments in the paramagnetic state have also been measured extensively.

In 1957, the first neutron experiments with polarization analysis was carried out by Nathans et al (2). The set up and main results of this unpublished work are reproduced in Fig.I. It was the study of neutron spin flip by the antiferromagnet Cr_2O_3 . The polarization in the scattered neutron beam was established by measurement of the transmission through a magnetized polycrystalline block of iron. As predicted by Halpern and Johnson (3), the polarization state of the neutron beam depends upon the angle β , as defined in Fig.I.

Then in 1969, the classic paper by Moon, Riste and Koehler (4) appeared which demonstrated the power of polarization analysis for inelastic as well as elastic neutron scattering. In particular, when a magnetic field H is applied parallel (HF) to the scattering vector Q , then all magnetic scattering is spin flip. In the configuration shown in Fig.2, this scattering appears in the flipper ON channel, which also contains the nuclear spin incoherent scattering (NSI) and all of the background. The straightforward way to eliminate these unwanted components is to take the difference between the intensity I for HF and that for a vertical field (VF), both with flipper ON (see table I).

$$I = (HF - VF) = \frac{1}{2} I_M$$

This is the method used extensively by Ziebeck, Brown and their collaborators (5) in a series of pioneering studies of 3d metals and compounds, including Fe, Ni and MnSi. They used, intentionally, very broad energy resolution so that the analyzer essentially integrates over ω giving $S(Q)$ directly. The measured intensities were put on an absolute scale by comparison with powder intensities. Recent work at Brookhaven (6-10) has focused on the development of a polarized beam spectrometer with sufficient energy resolution to give direct information about $S(Q, \omega)$. So far we have centered our effort in the neutron energy range 10 and 150 meV, with Heusler monochromator and analyzer.

Fig.2 depicts our standard triple axis spectrometer converted into one utilizing polarized incident beams as well as polarization analysis. Among the many technical problems to be resolved is the production of a polarized beam with adequate intensity. In fact, this is the reason why the powerful technique of polarization analysis has not yet realized its full potential. For the energy range 13-60 meV, we are now down about a factor of 20 in intensity using a fully polarized configuration as compared with our focusing pyrolytic graphite triple axis instrument. This drastic loss of intensity, however, is amply compensated in many experimental situations by the simplicity and uniqueness of this technique.

As emphasized by Ziebeck and Brown (5), it is very important to put the measured I_M into absolute units. This is simple in principle; but in practice it requires a great deal of effort and experience (7,8,9,11) to arrive at reliable values. We demonstrate two examples of our intensity calibrations, one using phonons and the other using powder lines. The example shown in Fig.2 utilizes phonon and magnon intensities (7). Actually these data are collected by unpolarized neutron beams to test out the reliability of using a few selected phonons for conversion. The other example given in Fig.3 is for polarization analysis of the scattering from a powder sample of MnF_2 . In this favourable case, one can attain the calibration accuracy of 5 %.

So far we have concerned ourselves with the use of polarized neutrons for studies of spin dependent cross sections. However, in 1972 Mezei (12) invented a novel application of a polarized beam, namely, neutron spin echo. This gives an extremely high energy resolution by measuring changes in the modulation of the neutron beam polarization caused by inelastic scattering. One example of the spin echo measurement will be given later.

II. 3d FERROMAGNETS

The first series of ferromagnets we have investigated by polarization analysis are the 3d metals. Despite extensive studies in recent years (13), the ferromagnetism in 3d metals has remained one of the least understood topics of condensed matter physics. The most interesting ferromagnets are, of course, Fe and Ni. We have addressed the basic questions concerning the paramagnetic scattering from these ferromagnets in our recent series of neutron scattering studies (7,8,10,14,15). We have presented a different interpretation from the picture of "persistent spin waves" above T_c , previously advocated by Lynn and Mowk (16,17) for Fe and Ni. The main conclusion of our study is that the scattering function $S(Q,\omega)$ follows a simple universal form for a surprisingly wide range of Q,ω and temperature.

However, because of the extremely high energy scale of the magnetic cross section of Fe and Ni (see the A values in Table II), it is nearly impossible to map out the entire scattering function $S(Q,\omega)$. On the other hand, some of the 3d metallic ferromagnets, such as Pd_2MnSn can easily be studied by the current neutron scattering technique, utilizing energy transfers of less than 50 meV. We will briefly describe the results of our polarized beam study (18) on Pd_2MnSn before presenting the more difficult investigation on Fe and Ni.

We have selected the intermetallic compound Pd_2MnSn (one of the Heusler family) because of its localized, ferromagnetic nature. The saturated value of the Mn moment is $4.2 \mu_B$ which is in good agreement with the value obtained from paramagnetic susceptibility measurements. The simplest form of the magnetic cross section is :

$$\frac{d^2\sigma}{d\omega d\Omega} = \gamma_0^2 f^2(Q) e^{-2W} S(Q, \omega) \quad (2)$$

$$S(Q, \omega) = M^2 \frac{\kappa_1^2}{\kappa_1^2 + q^2} \frac{1}{\pi} \frac{\Gamma}{\Gamma^2 + \omega^2} \frac{\omega/kT}{1 - e^{-\omega/kT}} \quad (3)$$

where κ_1 is the inverse correlation length and M is simply related to the static magnetic susceptibility χ by

$$M^2 = 12 K_B T \chi \quad (4)$$

The energy line width Γ is given by

$$\Gamma = A q^{2.5} f(\kappa_1/q) \quad (5)$$

when $f(\kappa_1/q)$ is the Résibois-Piette dynamical scaling function (19).

Typical examples of polarized beam data (HF - VF) for Pd_2MnSn are shown in Fig.4 and the resulting line width Γ , resolution corrected, is shown in Fig.5. The width at T_c follows the scaling formula Eq.5 closely till $\zeta=0.2$ and changes over to a more general function, $1 - \cos^2 \pi \zeta$, at high ζ . The most important result of this study is the disappearance of spin waves near the zone boundary at T_c . This is in marked contrast to the case of EuO reported by Mook (20). Since both EuO and Pd_2MnSn are considered to be good examples of localized moment ferromagnets, the likely cause of the different paramagnetic responses

near zone boundaries may be long range magnetic interaction in Pd_2MnSn and a small number of exchange interactions in EuO (21).

Now we turn to the more controversial topic of magnetic correlations in the itinerant ferromagnet Fe above T_c . As seen in Fig.6(C), the magnetic cross section follows closely the simple scattering function (see Eqs.3 and 5), as was the case with the localized ferromagnet Pd_2MnSn . This was a rather surprising result because the "propagating spin wave" above T_c (16) should have shown a pronounced peak around 10 meV (see arrow). Three profiles shown in Fig.6 demonstrate the power of polarization analysis. Fig.6(b) shows two cross sections flipper ON (mainly magnetic) and OFF (mainly nuclear) with horizontal field (HF). Obviously, only polarization analysis permits clean separation of the magnetic cross section near $\Delta E=0$. Although the data ON (HF) alone still have the uncertainty of the background the difference ON (HF-VF) eliminates this (Fig.6 c). We were forced to use rather poor collimation because of intensity considerations; the set up has, nevertheless, sufficient resolution to characterize magnons and phonons below T_c (Fig.6 a).

The overall magnetic scattering of Fe above T_c can be summarized schematically by the equi-intensity contours in Fig.7. The only modification needed from Eq.2 is a change over from pure Lorentzian to steeper function of ω at the tailend of the cross sec-

tion. We have done this by introducing the additional parameter α (8). Recent theoretical calculations (22), with no adjustable parameter, using renormalization methods give almost identical cross sections to ours. The picture of propagating spin waves, with definite dispersion curves, above T_c was derived by series of constant E scans. Then $\Delta q/q$ was converted into $\Delta E/E$ by the "dispersion" relation. Quite unexpectedly, the modified Lorentzians show relative sharp peaks in constant E scans; these peaks were interpreted as propagating spin waves. We conclude that the magnetic fluctuations in Fe above T_c follow closely the scaling functions (Eq. 3-5), just as Pd_2MnSn did, up $\zeta=0.2$ (25).

Near the zone boundaries, however, distinct signatures of itinerant nature within Fe show up in comparison with the localized ferromagnet Pd_2MnSn . The moments, obtained by energy integration of $S(Q, \omega)$, are put in absolute units and these can be compared directly with the d.c. susceptibilities at $\zeta=0$ as well as any theoretical calculations. As emphasized by Brown et al (23), the values near the zone boundaries of Fe are considerably smaller than the localized Heisenberg model predicts. This is shown in the insert of Fig.7; the localized model gives the cross section between the broken and dotted lines. Because of our reactor spectrum, the limit of our energy integration can not go beyond $\Delta E=80\text{meV}$. This may not be sufficient to map out the entire spectrum of Fe near this zone boundary. However, both the Grenoble (23) and Brookhaven (24) results are in good agreement in that the major cross sections

in Fe are confined to an energy range below KT_c . In conclusion, a considerable progress has been made in experimental characterization of 3d ferromagnets. More definite theoretical treatments for Fe, in particular $S(Q, \omega)$ near zone boundaries, are needed for the next step towards a full understanding of 3d magnets.

We have also utilized the polarization analysis for more difficult problems of paramagnetic scattering in Ni (7,14,15,25), the weak ferromagnet MnSi (26) as well as the high temperature phase of iron, γ Fe (9). All of these have relatively weak magnetic scattering due to smaller moments. We have combined both unpolarized and polarized techniques; the latter always plays the key role in crucial measurements. Now we moved on to more dilute magnetic systems, where the polarization analysis becomes the unique way to separate out magnetic scattering near $\Delta E=0$.

III. HEAVY FERMIONS

Recently we have been engaged in the concentrated effort to characterize the magnetic scattering from heavy Fermions. The discovery of superconductivity in heavy Fermion systems (27) has generated a great deal of excitement concerning the magnetic and superconducting properties of these materials, for example $CeCu_2Si_2$, UBe_{13} and UPt_3 . They are characterized by extraordinarily large specific heat coefficients γ at low temperature which corresponds to an effective electronic mass of $\sim 100 m_e$. They also show the large temperature dependent magnetic susceptibility χ : As pointed out by Fisk et al (28), there is a good correlation between large γ 's and large χ 's among many uranium compounds. The first aim of our experiments is to test whether similar correlation exists between γ and the quasi elastic line widths Γ (see Eq.3).

So far we have used the simple scattering function in Eq.3, which is a symmetric Lorentzian around $\Delta E=0$ at high temperatures, where $\omega \ll kT$ and the detailed balance factor (the last term in Eq.3) is nearly unity. At low temperature, however, the line shape defined by

$$S_Q(\omega) \propto \frac{\Gamma}{\Gamma^2 + \omega^2} \cdot \frac{\omega}{(1 - e^{-\omega/kT})} \quad (6)$$

is very asymmetric around $\Delta E=0$ and show a peak around finite energy transfer $\Delta E \approx \Gamma$. In more general cases where the magnetic cross sections contain additional inelastic terms, one can proceed

by converting the measured $S(Q, \omega)$ into the imaginary part of the susceptibility $\text{Im}\chi(Q, \omega)$ by

$$S(Q, \omega) = \frac{2}{\pi} \frac{1}{1 - e^{-\frac{\omega}{kT}}} \text{Im}\chi(Q, \omega) \quad (7)$$

Then the real part of the susceptibility can be derived through a Kramers-Kronig relation:

$$\text{Re}\chi(Q) = \frac{1}{\pi} \int \frac{\text{Im}\chi(Q, \omega)}{\omega} d\omega \quad (8)$$

This process permits us to assess whether the measured magnetic cross sections cover the major part of the spectral weight.

Fig.8 shows our polarized beam data (29) collected from a powder sample CeCu_2Si_2 . Though statistics are rather poor, one sees nonetheless an asymmetric quasielastic line at 10K, which becomes more symmetric at 80K. The line width Γ was estimated as 1 meV at 10 K and 5 meV at 80K. In addition there is a small inelastic peak around 32 meV. These peak positions are in good agreement with the results, previously reported by Horn et al (30), in time-of-flight measurements. However, the relative spectral weights of the quasielastic to 32 meV (crystalline field) excitations were not given previously. Only with the polarization analysis one can obtain directly the magnetic cross sections on top of large nuclear cross sections near $\Delta E=0$.

In order to compare with bulk susceptibility measurements, the data were converted to an absolute scale by comparing the total paramagnetic scattering to the intensity of the powder peaks from the sample (see ref.8 and 11). The susceptibility was then obtained by the use of Eq.7 and 8. The results of the calculations are compared with d.c. susceptibility measurements in Fig.9. Within the precision of the present measurements, it is seen that the neutron results are in good agreement with bulk susceptibility measurements. This conclusion is consistent with that reached from measurements (31) of the induced moment magnetic form factor of CeCu_2Si_2 . Horn et al find, on the other hand, that the susceptibility calculated from their neutron measurements is much larger than the bulk susceptibility, a result which was interpreted to indicate that CeCu_2Si_2 is a Kondo-like system. No noticeable effects were observed in neutron scattering experiments, which are directly connected with the onset of superconductivity.

Very recently, another polarized beam study of CeCu_2Si_2 was reported by Johnson et al (32). This was carried out at ILL with the technique developed by Ziebeck and Brown (5), utilizing a broad instrumental resolution of $2\Gamma(\text{Res}) = 43 \text{ meV}$. The observed profile at 6 K shows a single broad peak centered around 30 meV.

On the first glance, this result is entirely different from our profiles on Fig.8, where the larger of the two peaks is located near $\Delta E=0$. However, if one convolutes our two peak structure

with 43 meV resolution, one may obtain a single broad peak centered around 20 meV. The peak might shift to higher energies if there are significant cross sections beyond 40 meV. These higher energy excitations, however, contribute little to the susceptibility because they are weighted by $1/\omega$. So far no changes in the magnetic cross sections have been detected through the super conducting transitions at 0.5K.

In summary CeCu_2Si_2 has a very narrow line width $\Gamma \sim 1\text{meV}$ at low temperature and this quasielastic response carries the major spectral weight. In this sense, the expected correlation between γ (specific heat) at Γ (neutron) is satisfied. This is not the case with another heavy Fermion superconductor UPt_3 (34). As shown in Fig.10, the UPt_3 ingot shows a broad peak around $\Gamma=9\text{ meV}$ at 1.3 K and again, the $\chi(Q)$ obtained through Eq.8 are in reasonable agreement with the low temperature bulk susceptibility. In addition the Q dependence of this 9 meV peak shows intensity variation consistent with the uranium form factor, indicating that there are no strong correlations even at low temperatures.

Very recently, Buyers et al (34) have reported a very different type of magnetic scattering from single crystals UPt_3 . The spin fluctuations are broadly enhanced around (001) (zone boundary) and signify antiferromagnet correlation. The excitations are confined to the energy range below 1.5 meV and show a pre-

cipitous decrease of intensity around 1.5°K on cooling. These observations are interpreted to be consistent with the existence of a gap-like structure in the normal phase and the participation of spin fluctuations in the formation of the superconducting state below 0.5K. At present, it is not possible to assess the relative intensity of these low energy excitations to those around 9 meV reported by Aeppli et al (33).

Another heavy Fermion superconductor UBe_{13} ($T_c=0.9$ K) has been investigated recently by polarized and unpolarized neutron scattering measurements (11). The majority of the spectral weight is located in a broad quasielastic peak with $\Gamma=14$ meV. So far, no evidence of a narrow (~ 1 meV) f-level resonance predicted by the electronic specific heat is observed. This study was carried out with the powdered sample and the Q dependence of the magnetic intensity follows approximately the uranium form factor. Again, no detectable changes in intensities take place at T_c .

When we compare the polarized beam studies of 3d ferromagnets with those of heavy Fermions, the latter suffer two major intensity problems. One is the obvious fact that the heavy Fermions we have investigated are magnetically dilute systems. The second, probably more important factor is the lack of magnetic correlations

even at low temperatures; these correlation would enhance magnetic cross sections in narrow regions of Q space. The only exception, so far, is a weak antiferromagnetic coupling in UPt_3 discovered by Buyer et al (35). Further experiments are now underway on $CeCu_6$ and U_2Zn17 (antiferromagnet $T_N=10K$).

IV. CONCLUDING REMARKS

So far we have reviewed mainly the magnetic excitations studied by a triple-axis polarized beam set up. Our investigation is always combined with higher resolution unpolarized triple axis measurements. At the energy range of $10\mu eV$ or lower the novel ultra high resolution technique is now available. This is neutron spin echo technique of Mezei (12) which has recently been applied to spin dynamics of cubic ferromagnets (35). This technique uses the polarization of neutrons in an entirely different way from the regular polarization analysis. It is used simply to detect a small change of inelasticity, magnetic or non-magnetic, through the echo technique. One example is shown in Fig.11, where the most recent triple axis work (21) overlaps with the spin echo energy range. It is satisfying to see such a perfect agreement by two very different techniques.

ACKNOWLEDGEMENT

This article has been written for the ceremonial symposium of Professor C.G.SHULL'S seventieth birthday. It has been such a delightful experience for me to associate with Prof.SHULL for so many years, starting with the experiment shown in Fig.I of this paper. This review was prepared while I was a visiting scientist at HAHN MEITNER INSTITUTE on a HUMBOLDT fellowship. I would like to thank Prof.H.DACHS and all of his colleagues for warm hospitality during my stay in Berlin. I am also grateful for many stimulating discussions with G.Aeppli, P.Böni, A.I.Goldman, F.Mezei, A.Rollason, S.M.Shapiro and M.Steiner. The work at Brookhaven is supported by the Division of Material Science, U.S. Department of Energy under contract No.DE-AC02-76CH 00010.

REFERENCES

1. See, for example, R.Nathans, C.Shull, G.Shirane, and A.Andresen, Phys.Chem.Solids, 10 (1959) 138.
2. R.Nathans, T.Riste, G.Shirane, and C.G.Shull, Bull.Am.Phys.Soc. 2 (1957) 1, FA4 and unpublished.
3. O.Halpern and M.R.Johnson, Phys.Rev.55 (1939) 898.
4. R.M.Moon, T.Riste, and W.C.Koehler, Phys.Rev.181 (1969) 920.
5. K.R.A. Ziebeck and P.J. Brown, J.Phys.F10, (1980) 2015.
6. C.F.Majkrzak and G.Shirane, Jour. de Physique, Colloque C7 (1982) 215.
7. O. Steinsvoll, C.F.Majkrzak, G.Shirane, and J.Wicksted, Phys.Rev. B30 (1984) 2377.
8. J.P.Wicksted, P.Böni and G.Shirane, Phys.Rev.B30 (1984) 3655.
9. P.Böni, G.Shirane, and J.P.Wicksted, Phys.Rev.31 (1985) 4597.
10. G.Shirane, O.Steinsvoll, Y.J.Venmura, and J.Wicksted, J.App.Phys.55 (1984) 1887.
11. A.Goldman, S.M.Shapiro, G.Shirane, J.L.Smith, and Z.Fisk, Phys.Rev. to be published.
12. F.Mezei, Z.Physik 255 (1972) 146.
13. See, for example, the recent review articles by T.Moriya, J.Magn.Magn.Mater.14 (1979), 1; 31 (1983) 10.

14. P.Böni and G.Shirane, J.Appl.Phys. 57 (1985) 3012.
15. J.L.Martinez, P.Böni and G.Shirane,
Phys.Rev. to be published.
16. J.W.Lynn, Phys.Rev.B11 (1975), 2624; Phys.Rev. B 28,
(1983) 6550; Phys.Rev.Lett. 52 (1984) 775.
17. H.A. Mook, J.W. Lynn, and R.M. Nicklow, Phys.Rev.Lett. 30
(1973) 556; J.W. Lynn and H.A. Mook, Phys.Rev. B23
(1981) 198.
18. G. Shirane, Y.J. Uemura, J.P. Wicksted, Y. Endoh, and
Y.Ishikawa, Phys.Rev. B31 (1985) 1227.
19. R.Résibois and C.Piette, Phys.Rev.Lett.24 (1970) 514.
20. H.Mook, Phys.Rev.Lett.46 (1981) 508.
21. P.Böni and G.Shirane, Phys.Rev. to be published.
22. R.Folk and H.Iro, preprint 1985.
23. P.J. Brown, H. Capellmann, J. Déportes, D. Givord, and
K.R.A. Ziebec, J. Magn. Mater. 30 (1982) 243.
P.J. Brown, H. Capellmann, J. Déportes, D. Givord,
S.M. Johnson, J.W. Lynn, and K.R.A. Ziebeck,
J. de Physique, 46 (1985) 827.
24. G.Shirane, P.Böni, and J.P.Wicksted,
Phys.Rev. to be published.
25. The situation of Ni is still somewhat controversial.
See Refs. 14,15 and Mook and J.W.Lynn.
J.Appl.Phys. 57 (1985) 3006.

26. Y. Isikawa, Y. Noda, Y.J. Uemura, C.F. Majkrzak, and G. Shirane, Phys. Rev. 31 (1985) 5884.
27. See, for example, the recent review article by G.R. Stewart, Rev. Mod. Phys. 56, (1984) 755.
28. Z. Fisk, J.L. Smith, H.R. Ott, and B. Batlogg, J. Magn. Magn. Mater, to be published.
29. C.Stassis, B. Batlogg, J.R. Kemeika, J.D. Axe, G. Shirane, and Y. Uemura, Phys. Rev., to be published.
30. S. Horn, E. Holland-Moritz, M. Loewenhaupt, F. Steglich, H. Scheuer, A. Benoit and J. Flouquet, Phys. Rev. B23 (1981) 3171.
31. C. Stassis, J.D. Axe, C.F. Majkrzak, B. Batlogg, J.P. Remeika, J. Appl. Phys. 57 (1985) 3037.
32. S.M. Johnson, J.A.C. Bland, P.J. Brown, A. Benoit, H. Capellmann, J. Flouquet, H. Spille, F. Steglich, and K.R.A. Ziebeck, Z.Phys. to be published.
33. G. Aeppli, E. Bucher and G. Shirane (to be published).
34. W. J. L. Buyers, J. K. Kjems and J.D. Garrett (preprint 1985).
35. F. Mezei, J. Magn. Magn. Mater, 45 (1984) 67

T A B L E 1

Magnetic σ_M and nuclear σ_N neutron cross sections for the polarization analysis setup. E_f is fixed and the flipper is placed after the sample. Other notations are nuclear spin incoherent (NSI) and background (BG).

	Flipper on (+ -)	Flipper off (+ +)
Horizontal field	$\sigma_M + \frac{2}{3} \sigma_{NSI} + \sigma_{BG}$	$\sigma_N + 0\sigma_M + \frac{1}{3} \sigma_{NSI} + \sigma_{BG}$
Vertical field	$\frac{1}{2} \sigma_M + \frac{2}{3} \sigma_{NSI} + \sigma_{BG}$	$\sigma_N + \frac{1}{2} \sigma_M + \frac{1}{3} \sigma_{NSI} + \sigma_{BG}$

Table 2

Cubic Ferromagnets. In this Table A^* and κ_0^* are expressed in units of reduced wave number ζ of the inverse plane distance d^* . Note a narrow range of κ_0^* , in contrast to a very large variation of A^* . d^* corresponds to (110) for Fe and (111) for other ferromagnets. n is the number of important exchange constants J_n . After P. Böni and G. Shirane (21).

	Ni	Fe	Pd ₂ MnSn	EuO
T_c (°K)	627	1043	190	69.2
A (meV $\text{\AA}^{2.5}$)	350	140	60	8.3
$A^*(\zeta)$	5900	2400	230	53
A^*/T_c (K ⁻¹)	9.4	2.3	1.2	0.77
$\kappa_0^*(\zeta)$	0.20	0.34	0.22	0.30
lattice constant a (\AA)	3.5	2.9	6.4	5.2
$d^*(\text{\AA}^{-1})$	3.1	3.1	1.7	2.1
n			> 6	= 2

$$\Gamma = Aq^{2.5} \text{ at } T_c, \quad \kappa_1^* = \kappa_0^* \left(\frac{T-T_c}{T_c} \right)^{0.7}$$

FIGURE CAPTIONS

Fig.1 (a) Schematic diagram of the experimental arrangement used in determining the neutron polarization after crystal scattering.

(b) The polarization in the scattered beam from Cr_2O_3 as a function of the angle β for different temperatures. After Nathans, Riste, Shirane, and Shull (2).

Fig.2 The left side is the calibration curve for unpolarized neutron scattering from ^{60}Ni . The right side shows a schematic diagram of a triple-axis spectrometer in the polarized neutron mode. After Steinsvoll et al (7).

Fig.3 Paramagnetic scattering from powder MnF_2 (12 mm cylinder) with polarization analysis. Powder intensities (see insert) converts these magnetic cross sections to absolute units. After Goldman et al (11).

Fig.4 Examples of magnetic scattering from the localized, metallic ferromagnet Pd_2MnSn near its Curie temperature $T_c=193^\circ\text{K}$. After Shirane et al (18).

Fig.5 The linewidth Γ for the entire zone of (111) in the Heusler compound Pd_2MnSn . After Shirane et al (18).

Fig. 6 (a) "Unpolarized" neutron study of Fe at $T=T_C-322$ K.
(b) Polarized beam study at $T=1.02 T_C$ with horizontal magnetic field (HF). Open circles are data with flipper ON (mainly magnetic), and the dashed curve illustrate data with flipper OFF (mainly nuclear).
(c) Polarized beam data: horizontal (HF) and vertical field (VF) difference with flipper ON.
After Wicksted et al (8).

Fig.7 Magnetic cross sections of pure Fe at $T=T_C+22^\circ\text{K}$. Intensity contours are represented by model calculations. After Wicksted et al (8).

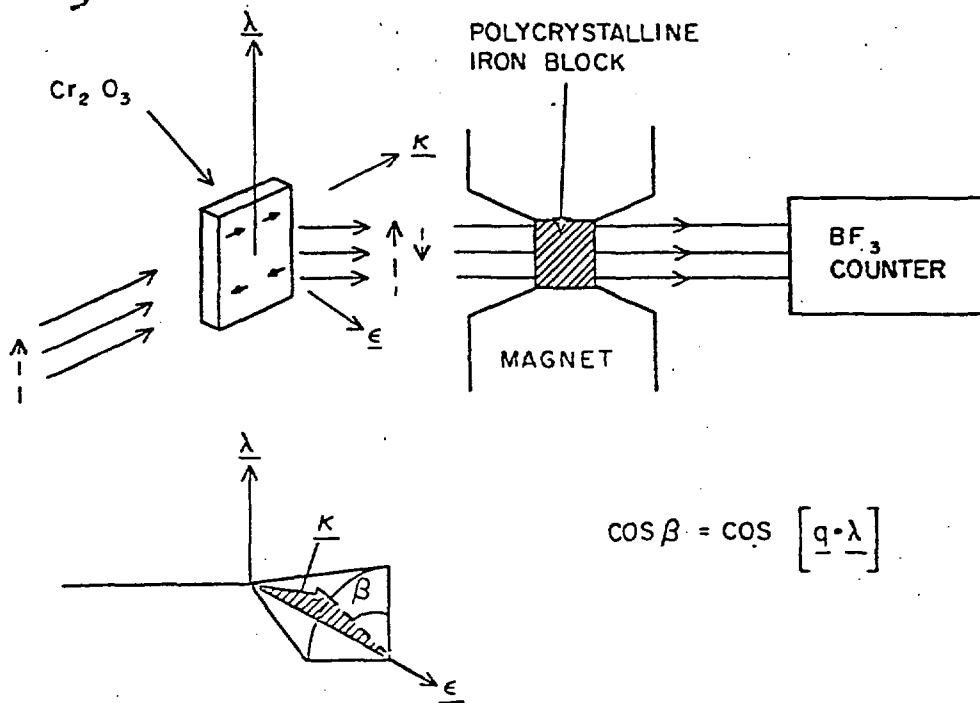
Fig.8 Energy distribution of the paramagnetic scattering (at $Q=2\text{\AA}^{-1}$) from CeCu_2Si_2 . After Stassis et al (29).

Fig.9 Comparison of the susceptibility values obtained from the neutron scattering measurements with the bulk susceptibility of CeCu_2Si_2 . After Stassis et al (29).

Fig.10 Constant Q spectra of UPt_3 at 1.3°K . After Aeppli et al (33).

Fig.11 Linewidth versus q of EuO in a log-log representation. The spin echo data by Mezei (35) and triple axis data by Böni and Shirane (21) follow perfectly the dynamical scaling prediction $\Gamma=Aq^{2.5}$ over 4 decades in energy.

a)



b)

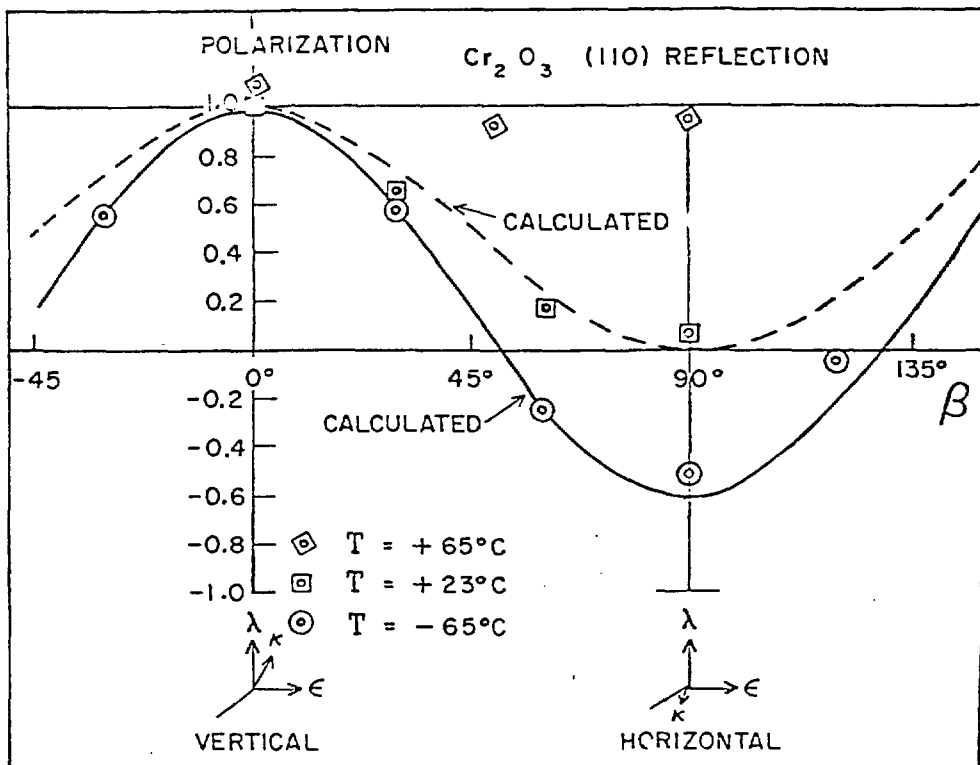


FIGURE 1

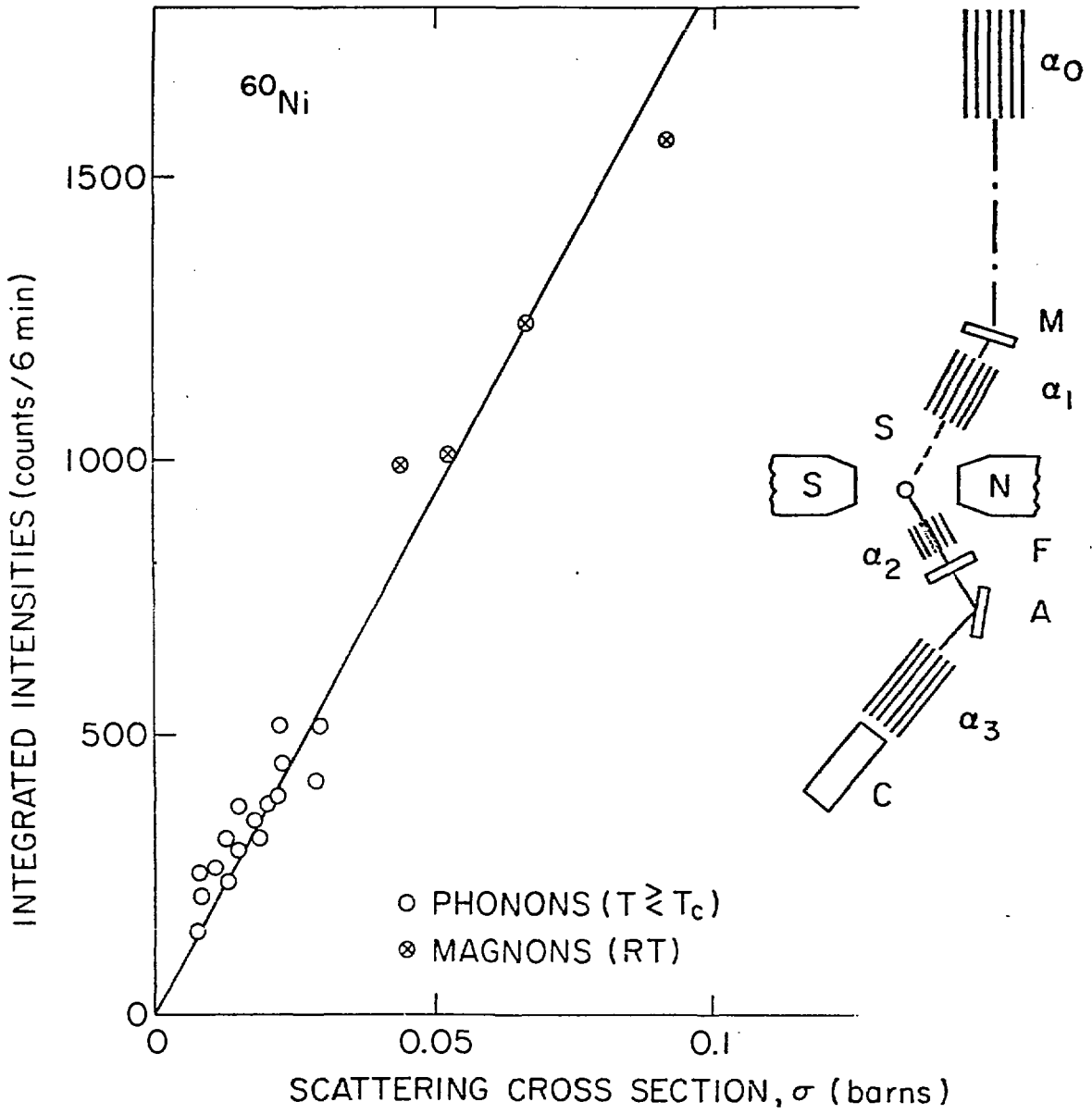
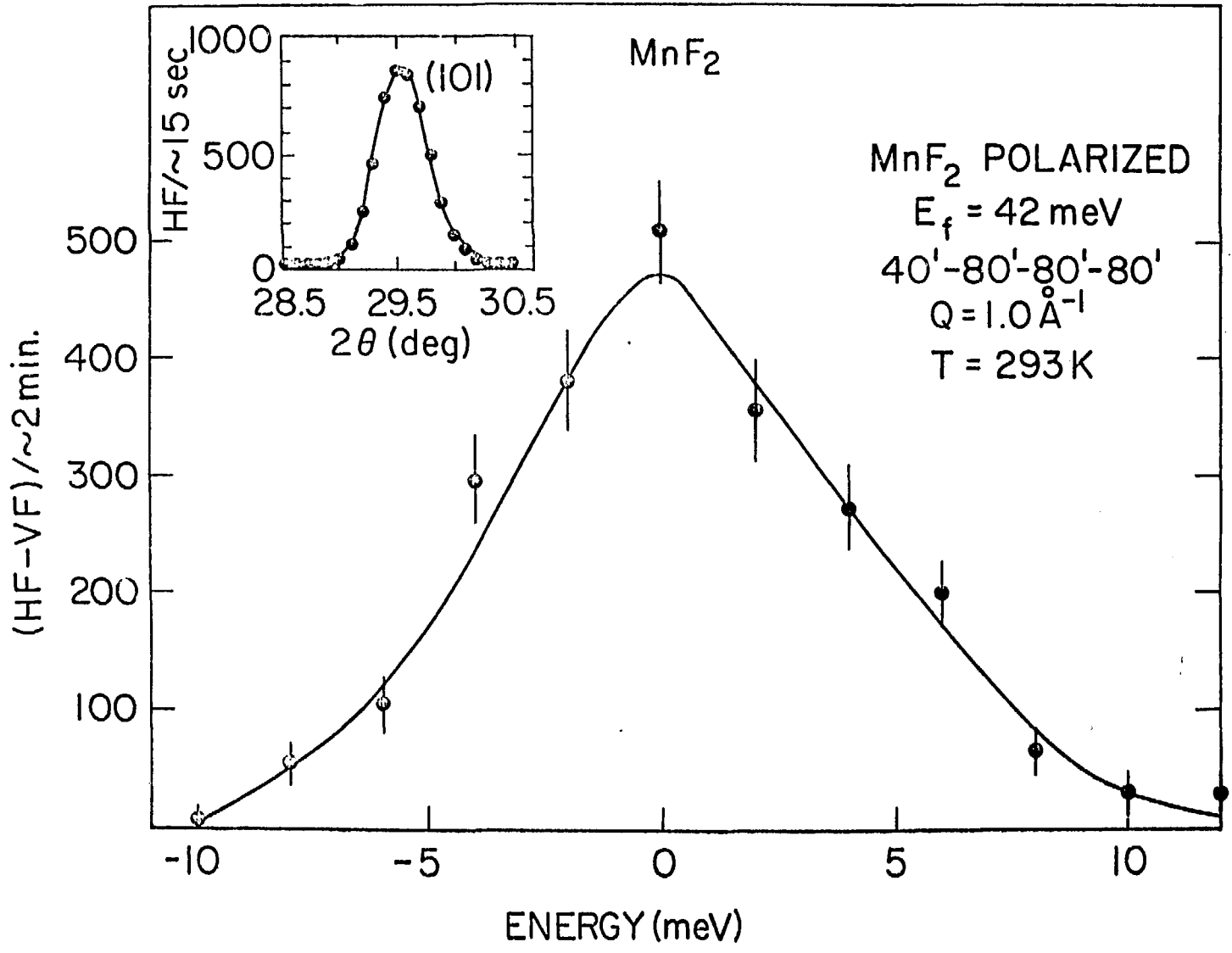


FIGURE 2

FIGURE 3



Pd₂ Mn Sn 30.5 E_f 40'-80'-80'-80'

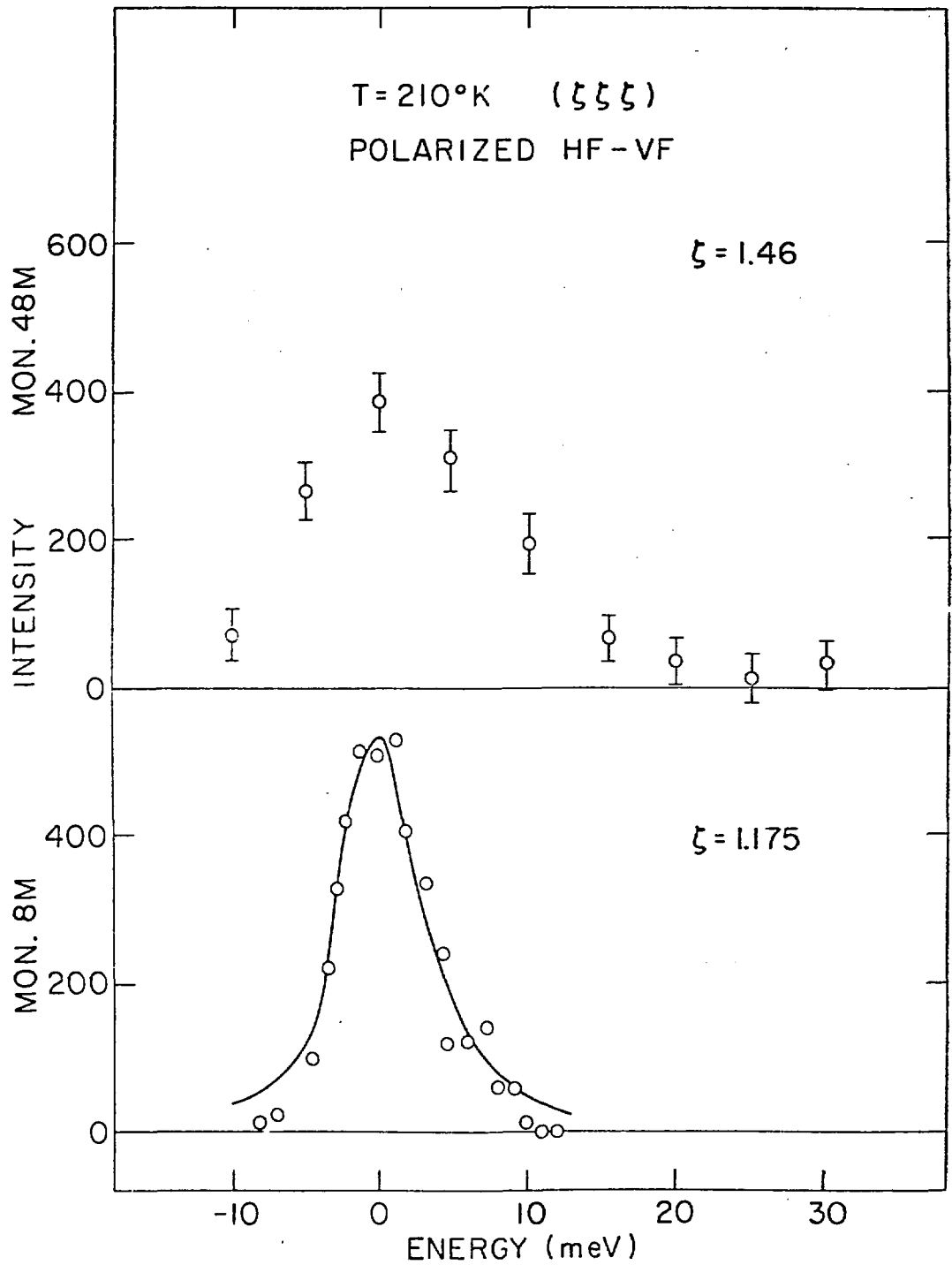


FIGURE 4

Pd₂MnSm T = 210°K

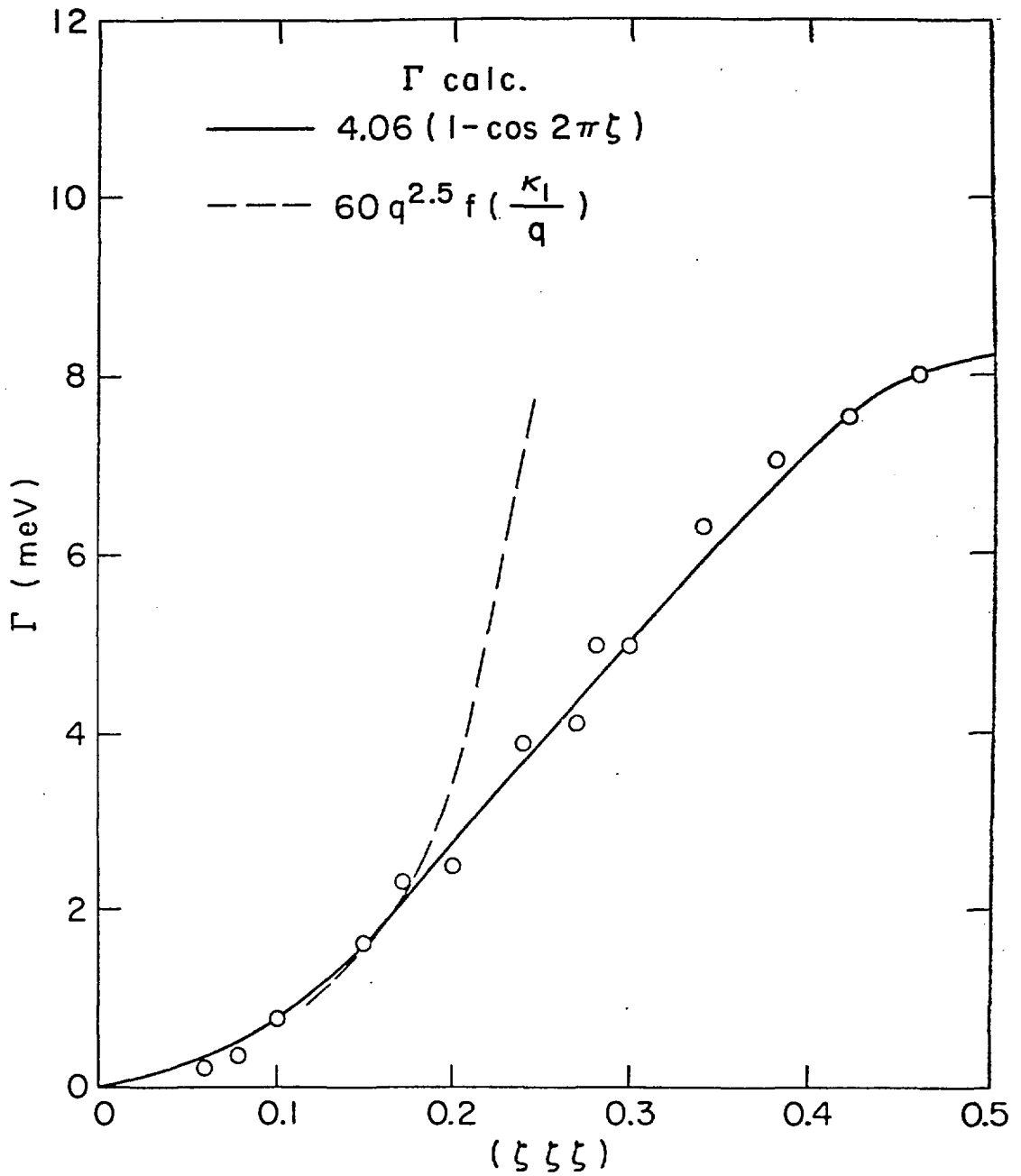


FIGURE 5

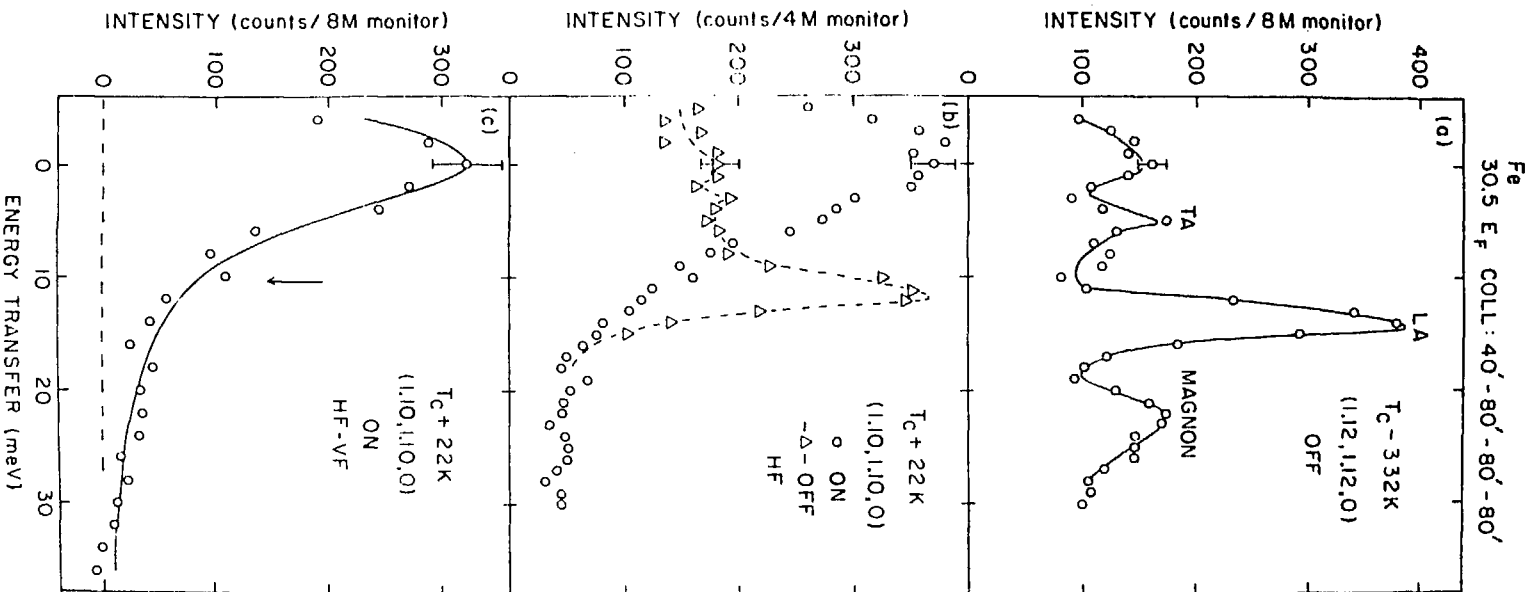


FIGURE 6

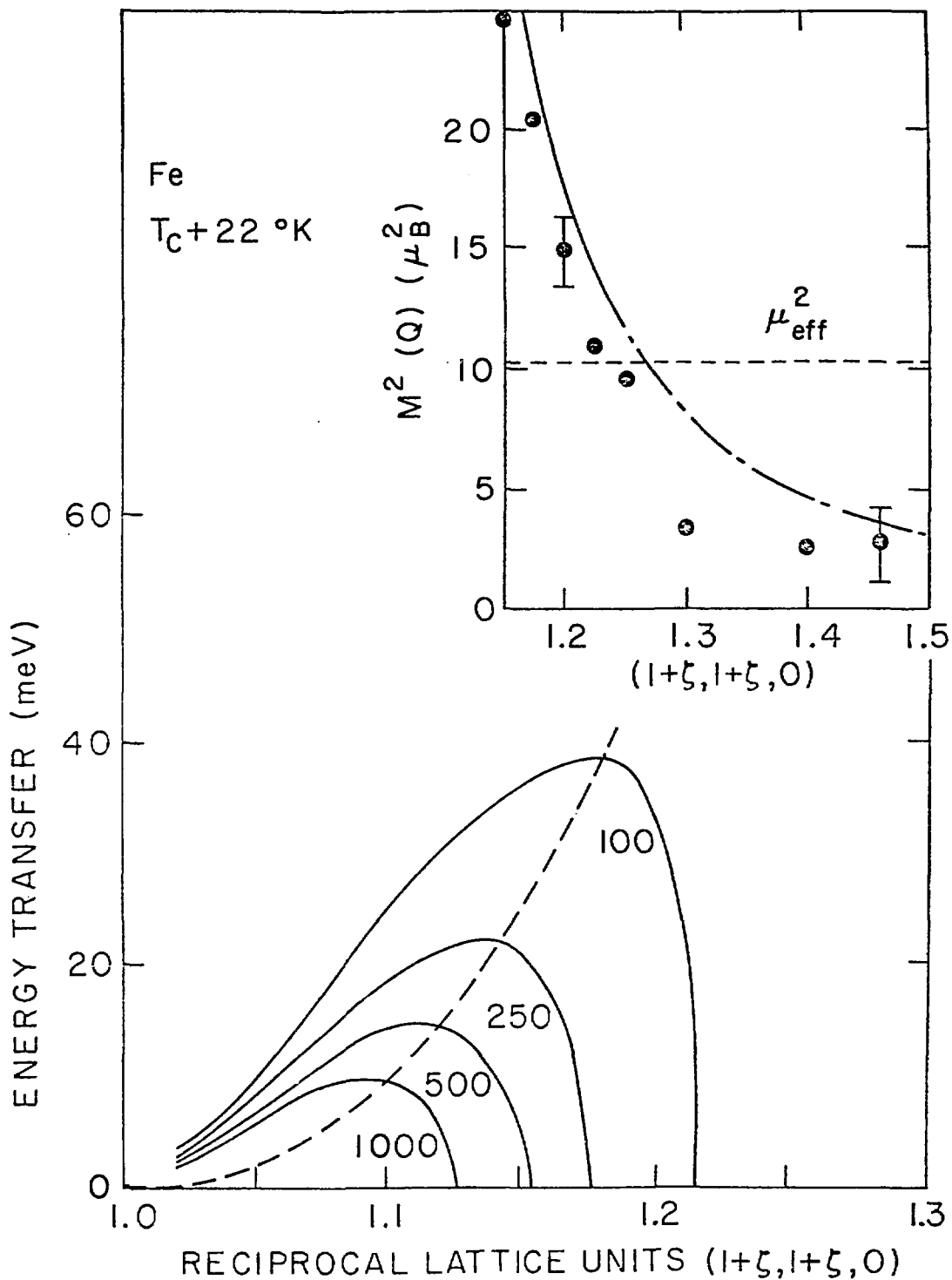


FIGURE 7

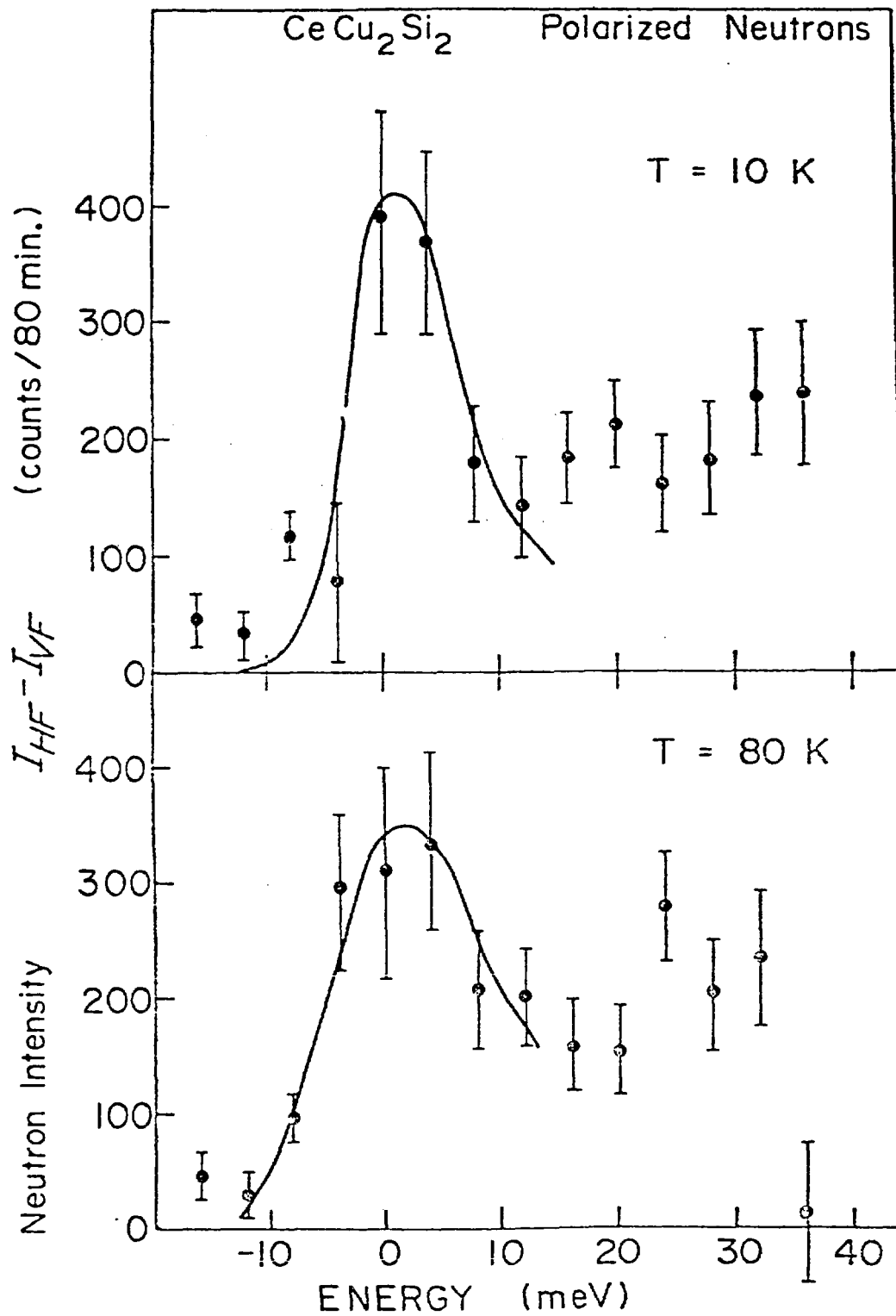


FIGURE 8

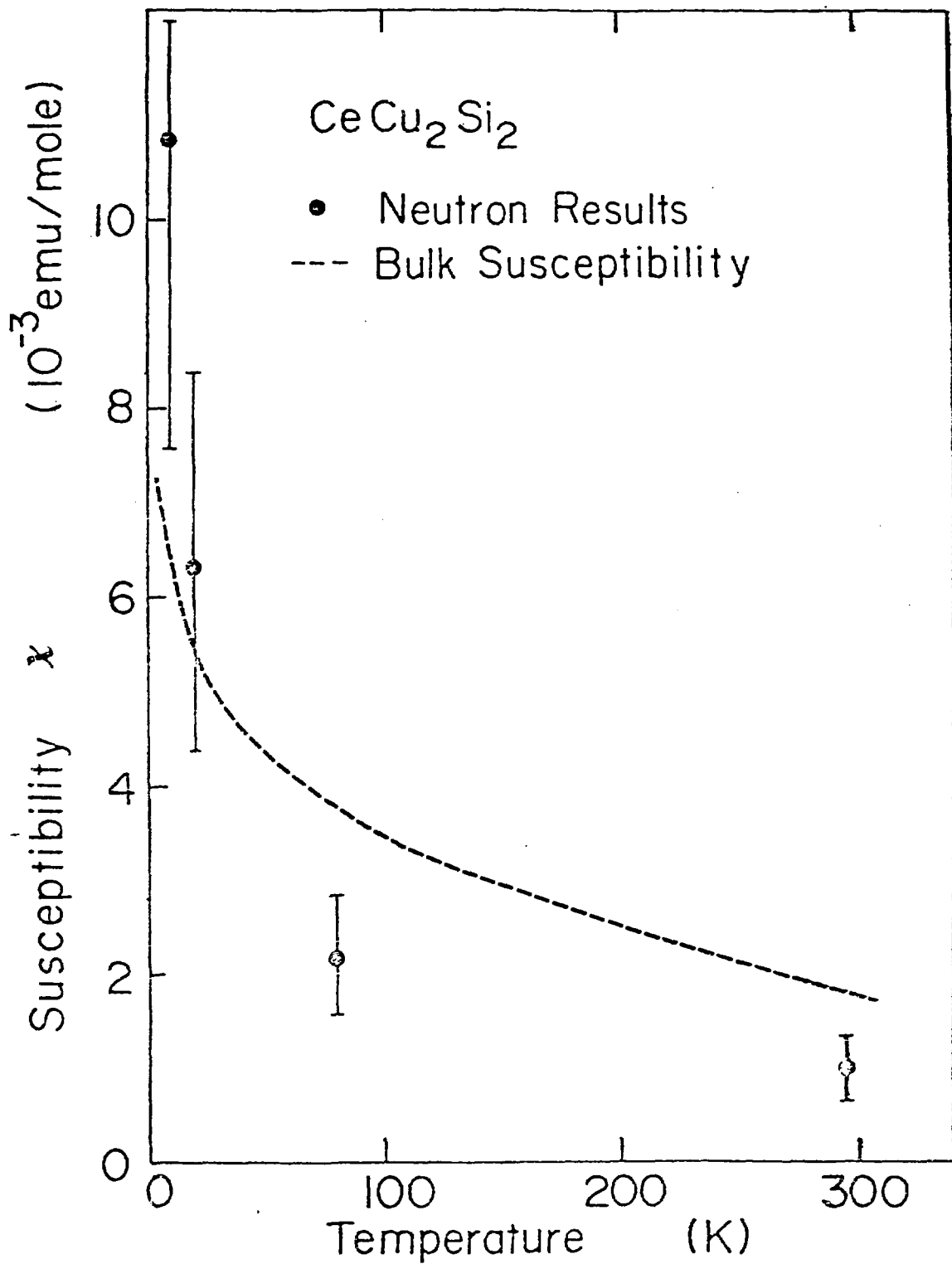


FIGURE 9

UPt₃ POLARIZED BEAM

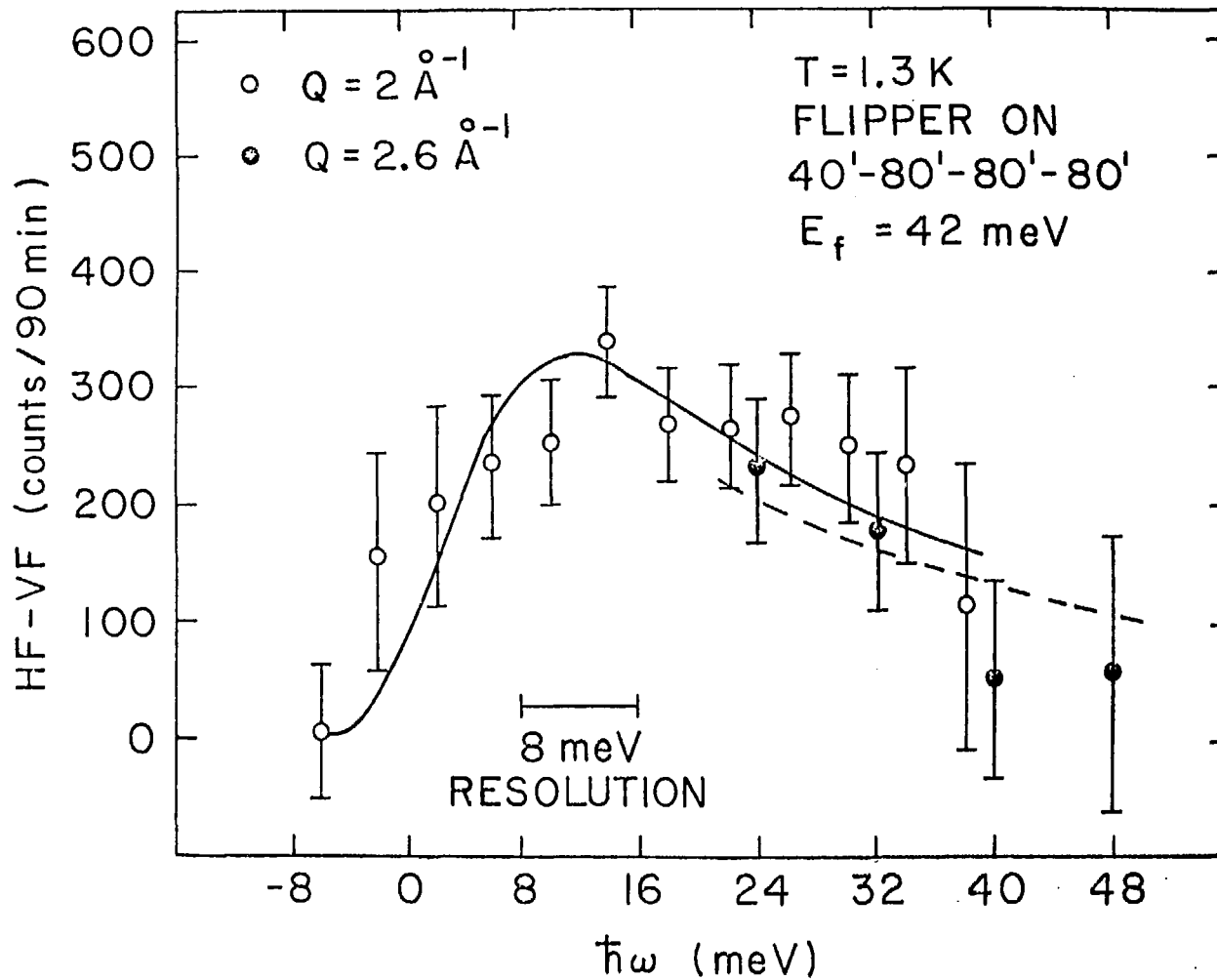


FIGURE 10

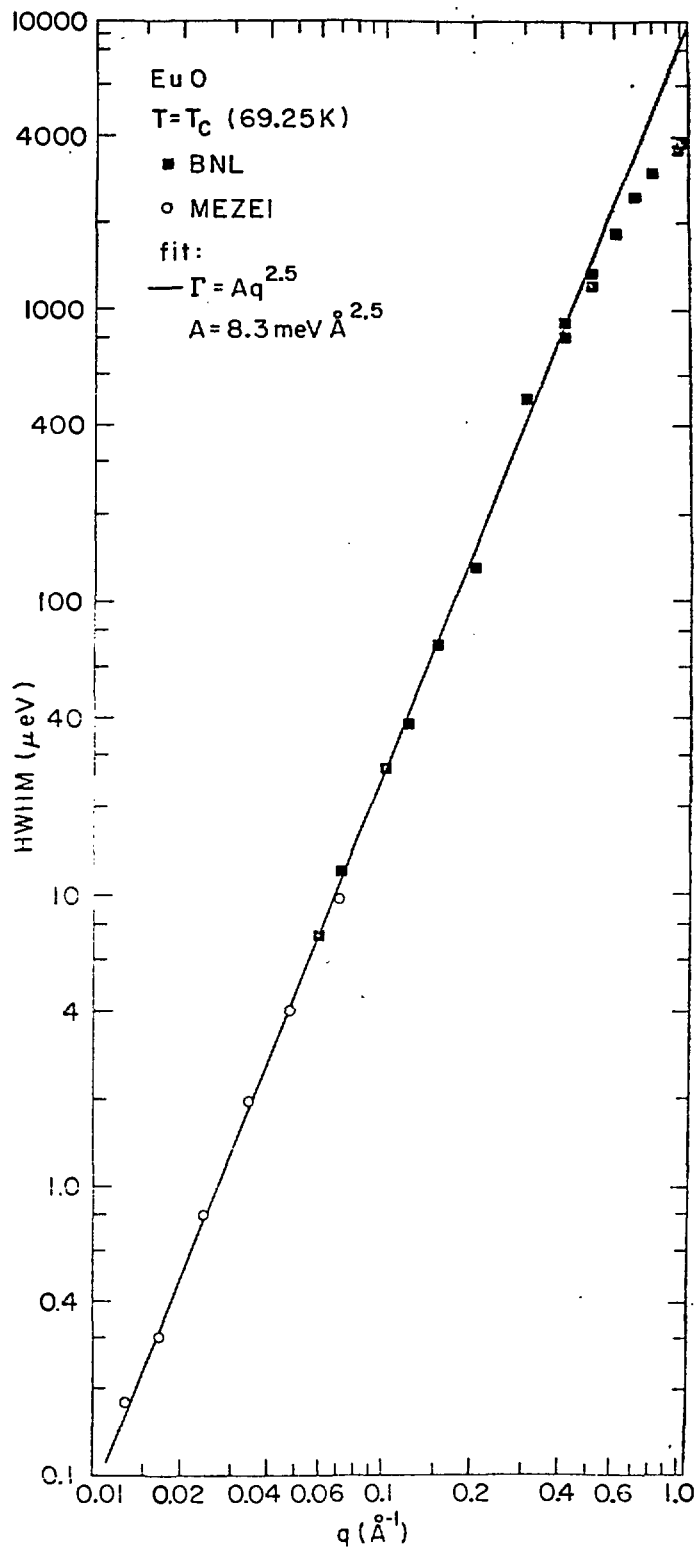


FIGURE 11